Ultrasonics Sonochemistry 89 (2022) 106152

Contents lists available at ScienceDirect

Ultrasonics Sonochemistry

journal homepage: www.elsevier.com/locate/ultson

Hybrid solvothermal/sonochemical-mediated synthesis of ZnO NPs generative of ˙OH radicals: Photoluminescent approach to evaluate ˙OH scavenging activity of Egyptian and Yemeni *Punica granatum* arils extract

Amr A. Essawy [a,b,*], Ibrahim B. Abdel-Farid [c,d]

[a] Chemistry Department, College of Science, Jouf University, Sakaka P.O. Box 2014, Saudi Arabia
[b] Chemistry Department, Faculty of Science, Fayoum University, 63514 Fayoum, Egypt
[c] Biology Department, College of Science, Jouf University, Sakaka P.O. Box 2014, Saudi Arabia
[d] Botany Department, Faculty of Science, Aswan University, Aswan, Egypt

ARTICLE INFO

Keywords:
Solvothermal/sonochemical synthesis
ZnO NPs
Solar-illumination
Fluorimetric probing
Hydroxyl radicals scavenging
Pomegranate arils

ABSTRACT

Zinc oxide NPs were synthesized solvothermally within sonochemical mediation and characterized by XRD, FTIR, SEM, EDX, elemental mapping, TEM and UV–vis. spectrophotometry. To evaluate the hydroxyl radicals (˙OH) scavenging activity of arils extract of Egyptian (EGY-PAM) and Yemeni *Punica granatum* (YEM-PAM), the developed zinc oxide nano particles (ZnO NPs) as a highly productive source of hydroxyl radicals (under Solar-illumination) was used. The yield of ˙OH was trapped and probed via fluorimetric monitoring. This suits the first sensitive/selective photoluminescent avenue to evaluate the ˙OH scavenging activity. The high percentage of DPPH radical scavenging reflected higher contents of phenolics, flavonoids, and anthocyanins that were found in EGY-PAM and YEM-PAM. Although, some secondary metabolites contents were significantly different in EGY-PAM and YEM-PAM, the traditional DPPH radical scavenging methodology revealed insignificant IC_{50}. Unlike, the developed fluorimetric probing, sensitively discriminated the ˙OH scavenging activity with IC_{50} (105.7 μg/mL) and lower rate of ˙OH productivity ($k = 0.031\ min^{-1}$) in case of EGY-PAM in comparison to IC_{50} (153.4 μg/mL) and higher rate of ˙OH productivity ($k = 0.053\ min^{-1}$) for YEM-PAM. Our findings are interestingly superior to the TBHQ that is synthetic antioxidant. Moreover, our developed methodology for fluorimetric probing of ˙OH radicals scavenging, recommends EGY-PAM as ˙OH radicals scavenger for diabetic patients while YEM-PAM exhibited a better ˙OH radicals scavenging appropriate for high blood pressure patients. More interestingly, EGY-PAM and YEM-PAM exhibited high anticancer potentiality. The aforementioned ˙OH and DPPH scavenging activities as well as the anticancer potentiality present EGY-PAM and YEM-PAM as promising sources of natural antioxidants, that may have crucial roles in some chronic diseases such as diabetics and hypertension in addition to cancer therapeutic protocols.

1. Introduction

Photoexciting semiconductor metallic oxide nanoparticles could generate hydroxyl radicals (˙OH) by moving electrons from the valence band to the conduction band, leaving behind a photogenerated hole (h^+). That holes could combine with water molecules and/or hydroxide ions to make ˙OH radicals [1–3]. The amount of photocatalytically-generated ˙OH radicals could be correlated to semiconductor type, morphology, structurality, and optical properties [4,5]. The semiconductor, Zinc oxide (ZnO) has gained popularity because it is environmentally sustainable of non-toxic chemistry and low cost. A number of physical properties change when microparticles become nanoparticles. The two most important of these are an increase in surface area-to-volume ratio and a reduction in particle size [6].

Hydrothermal, sol–gel, combustion, and Co-precipitation are among methods used to synthesize nanoparticles [7–10]. Ultrasonic irradiation during particle synthesis affects material structure and morphology [11]. Ultrasonic micro-bubbles improve chemical reactions in solution [12]. The growth and collapse of micro-bubbles transmits sonic energy to vapour [13]. During the bubble's vapour phase collapse, pressure and temperature rise. This creates many reactive free radicals [14]. This exclusive energy causes aqueous compound reactivity. Nanoparticles

* Corresponding author at: Chemistry Department, College of Science, Jouf University, Sakaka P.O. Box 2014, Saudi Arabia.
E-mail address: aae01@fayoum.edu.eg (A.A. Essawy).

https://doi.org/10.1016/j.ultsonch.2022.106152
Received 11 June 2022; Received in revised form 25 August 2022; Accepted 28 August 2022
Available online 29 August 2022

possess catalytic properties where those of small size and high active surface increase catalytic efficiency. Ultrasonic irradiation improves particle size and uniformity [15]. Sharifalhoseini et al. [16] studied sonicating ZnO nanoparticles where the applied sonication improved particle structure and antibacterial properties in addition to the influence of ultrasonic intensity on particle morphology. Ultrasonic irradiation has a significant effect on purifying ZnO nanoparticles, and cavitation is the main reason for particle morphology changes [17]. The aforementioned merits play pivotal role in photogenerating ˙OH radicals with high efficiency from photoexcited ZnO.

Hydroxyl radical (˙OH) belongs to intracellular reactive oxidizing species (ROS) that are mainly generated from oxygen via electron transfer providing a viable coding operators for cellular processes and the maintenance of redox equipoise for cell propagation and discrimination [18,19]. ˙OH radicals gain specific attentiveness because of its sturdy reactivity of quite short half-life time ($\sim 10^{-9}$s) and interaction with other molecules with high rates (10^{9}–10^{10} $M^{-1}s^{-1}$) [20], in addition to its potent oxidizability within 2.31 V reduction potential [19]. In cells, ˙OH is catalytically generated from H_2O_2 in presence of Fe^{2+} or Cu^{+}. Hydroxyl radicals is presumed as a deleterious species that could stimulate lipid peroxidation [21], oxidative damage of DNA bases and proteins [22] inducing pathophysiological processes of cardiovascular disorder, cancer, and inflammation [23].

Various technicalities have been developed to detect ˙OH such as electrochemical methods [24], absorption spectrophotometry [25], electron spin resonance (ESR) spectroscopy [26], chemiluminescence (CL) [27], high-performance liquid chromatography (HPLC) [28], and spectrofluorimetry [29]. Sophisticated instrumentation in ESR, operational complexity in HPLC, poor selectivity in CL, low sensitivity in spectrophotometry, low reproducibility in electrochemistry delimits these methods [30]. Merits of low cost, simplicity, high sensitivity and selectivity favor the usage of spectrofluorimetry over the aforementioned techniques for assaying ˙OH [31,32].

In addition to the necessity of sensitively monitoring ˙OH, seeking for antioxidants that enable the neutralization of ˙OH radicals by provisioning them with electrons to prevent or delimits the chain reactions responsible for tissue damage is also an imperious demand [33]. Many strong synthetic antioxidants such as butylated hydroxyltoluene (BHT) and butylated hydroxyanisole (BHA) are used in food industries [34]. These synthetic antioxidants are associated with many dangerous side effects such as liver damage and cancer induction [35]. Alternatively, scientists have started to use natural and safe antioxidants such as phenolics and flavonoids that are extracted from plants in food industries to enhance the antioxidant defenses and reduce the oxidative damage to human body [36].

Punica granatum L. commonly known as pomegranate is a woody perennial shrub and sometimes small tree belongs to the family Lythraceae. It is native to Persia and has been extensively cultivated in the Mediterranean countries including Tunisia, Turkey, Egypt, Spain, USA, China, Japan, and Russia [37–39]. This plant has several bioactive secondary metabolites including polyphenols, fatty acids and volatile compounds [40–45]. The high contents of polyphenols in seeds extract of pomegranate was reflected in its antioxidant activity [40] that may be attributed to its high content of polyphenolics such as chlorogenic acid, coumaric acid, pyrogallol and rutin. The most important bioactive phenolic acid in pomegranate is the ellagic acid as it has many biological activities such as anticancer activity [46], antidiabetic, anti-inflammatory, anti-allergic, and antibacterial activities [47].

In this work, we aimed to suit the first integrated protocol for selective assaying of the scavenging potentiality of ˙OH radicals by the arils extract from Egyptian and Yemeni *Punica granatum* (EGY-PAM, YEM-PAM). The protocol started with the employment of a hybrid solvothermal/sonochemical route to synthesize ZnO NPs of better photoresponsive efficacy, to be suited in a solar-driven/fluorimetric probing system to selectively photogenerate and sensitively assay ˙OH radicals. Secondly, we examined the antioxidant efficacies of the EGY-PAM and YEM-PAM in scavenging ˙OH. In addition, the anti-proliferative activity is investigated.

2. Experimental

2.1. Materials

Fruits of two varieties (one from Yemen and another from Egypt) of *Punica granatum* were purchased from the market in Aljouf region, City of Sakaka, Saudi Arabia. Zinc acetate dihydrate ($Zn(CH_3COO)_2{\cdot}2H_2O$), benzyl alcohol, sodium hydroxide, terephthalic acid, ethanol, *tert*-butylhydroquinone (TBHQ), 2,2-Diphenyl-1-picryl-hydrazyl (DPPH), hydrochloric acid, sulforhodamine B (SRB), ascorbic acid, and catechol were obtained from Sigma Aldrich Chemical Co. (St. Louis, Mo, USA). All reagents were of analytical grade and were used as received. Deionized (DI) water was used to prepare all the working aqueous solutions.

2.2. Methods

2.2.1. Extracting of pomegranate arils (PA) molasses.

The fresh fruits of Egyptian and Yemeni *Punica granatum* were washed with tap water followed by deionized water to remove any dusty grains. Then the arils were collected, purified from other pulp contents. Exactly 500 g of each arils category were placed in 1.0 Liter Pyrex beaker and subjected to 4 days soaking in ethanol/water (80:20 % v/v). After that, the color of ethanol/water extracting mixture renders red. The extracted arils solution was filtered to remove possibly present sediments and exposed to rotary evaporation at 50 °C until getting the proper textures of pomegranate arils molasses (PAM) of the Egyptian and Yemeni origins denoted respectively as EGY-PAM and YEM-PAM. These extracts were stored at RT and kept in dark till the determination of their bioactive polyphenolics secondary metabolites such as total phenolics, flavonoids, and anthocyanins. Moreover, these extracts were used for evaluation of hydroxyl and DPPH radical scavenging activity as well as the reducing power and anti-proliferative activity against two carcinogenic cell lines (hepatocellular carcinoma and breast cancer cell lines).

2.2.2. Quantitative determination of metabolites by spectrophotometer

Determination of total phenolics: Folin-Ciocalteau method was used to estimate the total content of phenolics in *P. granatum* arils extracts [48].

Determination of flavonoids: Aluminum chloride was used to determine flavonoids content in the crude extract of *P. granatum* arils. The absorbance of samples and the standard (quercetin) were measured at 510 nm [49]. The content of flavonoid contents were expressed as quercetin equivalent (mg QE/g extract).

Determination of anthocyanins: Crude extracts of the *P. granatum* were dissolved in acidified methanol in brown tubes or in well closed tubes covered with aluminum foil and incubated at + 4 °C for 24 h [50]. The absorbance of the supernatants after centrifugation was recorded at 530 and 657 nm. The anthocyanins content was calculated using the following equation:

$$\text{Anthocyanin content } (\mu\text{mole/g}) = ([A_{530} - 0.33 \times A_{657}]/31.6) \times (\text{volume [mL]/weight [g]}) \quad (1)$$

Determination of reducing power (RP): Reducing power of different concentrations of ethanol extracts were determined based on Oyaizu 1986 in presence of phosphate buffer, potassium ferricyanide, chloroacetic acid and ferric chloride. The absorbance of the solution was read at 700 nm where ascorbic acid was used as positive control [51].

Determination of DPPH free radical scavenging activity assay: The extracts were vigorously shaken with a mixture of acetic acid solution (pH 5.5), ethanol aqueous solution (50 %) and DPPH in ethanol. The mixture was incubated for 30 min at RT protected from light. Different

concentrations of ascorbic acid, positive and negative controls were similarly treated as above [52]. The absorbance was read at 517 nm and the % inhibitions were plotted against concentrations where IC_{50} was calculated from the graph. The experiment of DPPH was performed in duplicates.

2.2.3. Cancer cell lines, medium and in vitro anticancer activity

Human hepatocellular carcinoma HepG-2 and breast cancer cell lines (MCF7) were obtained from an American Type Culture Collection (ATCC). PRMI-1640 medium supplemented with 10 % foetal bovine serum (FBS), 2 mL glutamine containing 100 U/mL streptomycin and 100 U/mL penicillin at 37 °C/5 % CO_2 were used for cell culturing.

2.2.4. Determination of inhibition concentration 50 % (IC_{50}) for P. Granatum extracts using sulforhodamine B (SRB) colorimetric assay

The antiproliferative activity of *P. granatum* extracts was evaluated using the sulforhodamine B colorimetric assay (SRB) by following a previously reported method [53,54].

2.2.5. Preparation of zinc oxide nanoparticles (ZnO NPs)

In 100 mL round flask, 4.0 g of zinc acetate dihydrate ($Zn(CH_3COO)_2{\cdot}2H_2O$) was added to a (1:10 v/v) solution of absolute ethanol and benzyl alcohol. The obtained mixture was subjected to hybrid refluxing system mediated with ultrasonication bath operated at 38 kHz ± 10 % frequency with 110 W output power and allowed solution heating at 80 °C for 3 h where a white precipitate is formed within evolution of ester smell. The precipitate was collected, washed 3 times with ethanol followed by 3 times washing with deionized water. The precipitate was firstly dried at 70 °C for 10 h and finally calcined at 450 °C for 2 h.

2.2.6. Solar-driven generative approach of hydroxyl radicals (˙OH) from ZnO NPs and spectrofluorimetric monitoring

The productivity of the developed ZnO NPs for the hydroxyl radicals (˙OH) under solar illumination were spectrofluorimetrically assayed due to the photoluminescence (PL) technicality [1]. In a representative methodology, 12.0 mg of the developed ZnO NPs was added to 40 mL of terephthalic acid, TA (0.005 mol/L) mixed with NaOH (0.01 mol/L). This mixture was illuminated by solar radiation of 3.75×10^4 Lux (recorded via PeakTech®digital multi tester). At a given time of illumination, about 5 mL of illuminated solution was withdrawn and centrifuged to remove any suspended ZnO NPs where the efficacy to breed ˙OH radicals is assayed by recording the distinguishing fluorescent peak of the produced hydroxy terephthalate fluorphore at emission wavelength 426 nm.

2.2.7. The potentiality in scavenging ˙OH radicals activity due to EGY-PAM or YEM-PAM

The potentiality of EGY-PAM or YEM-PAM in scavenging ˙OH radicals was addressed and compared using the spectrofluorimetric probing technicality. As aforementioned in section 2.2.6, the ascribed mixture in breeding ˙OH radicals under solar illumination was prepared where different amounts (90, 110, 155, and 220 μg/mL) of EGY-PAM or YEM-PAM were dissolved before starting the illumination process.

The scavenging percentage of hydroxyl radicals was estimated from the equation:

$$\text{Scavenging activity}\,(\%) = \left[\frac{(F_0 - F_s)}{F_0}\right] \times 100 \qquad (2)$$

where F_0 and F_s are respectively, the maximum fluorescence intensity of the formed fluorescent probe at λ_{em} 426 nm. in absence and presence of antioxidant samples at the same illumination time for the ˙OH radicals breeding system. Experiments were repeated three times where results were plotted as the scavenging activity percentage versus examined samples concentrations.

Moreover, addressing of the hydroxyl radicals scavenging potentialities due to EGY-PAM or YEM-PAM was employed in presence of high levels of glucose (5 mg/mL) and NaCl (15 mg/mL) by following the above procedures for breeding and selective fluorimetric probing of ˙OH radicals.

Furthermore, the efficacy of the studied samples for ˙OH radicals scavenging were kinetically examined by comparing the rates of breeding ˙OH radicals in absence and presence of antioxidant samples due to the equation:

$$\ln(F/F_o) = a + kt \qquad (3)$$

where F and F_o are respectively, the fluorescence intensity of the formed fluorescent probe at λ_{em} 426 nm. in presence and absence of antioxidant samples at illumination time (t) for the ˙OH radicals breeding system.

2.3. Statistical analysis

The statistical differences among the content of secondary metabolites in the two varieties of *P. granatum* (Egyptian and Yemen) was evaluated using analysis of variance (ANOVA) from Minitab (version 12.21) (difference at $p < 0.05$ was considered to be statistically significant).

2.4. Instruments

Absorption spectra within the UV–visible range were recorded utilizing the spectrophotometer Agilent Cary-60. While a Shimadzu IR Affinity-1S spectrometer was used for measuring the FTIR spectra. The XRD spectra were employed using D/Max2500VB2/*Pc*-X-ray diffractometer (Rigaku, Tokyo, Japan) with a Cu detector X-ray of wavelength 1.54 Å. The TEM imaging of sample was depicted utilizing the electron microscopy (JEOL, JEM-2100, Japan). Zeiss FESEM Ultra 60 field emission scanning electron microscopy with EDX and mapping analyses was used to examine the morphological characteristics of the developed material. The photoluminescence measurements were recorded by using Agilent fluorimeter and the Guyson ultrasonic bath (MKC6) operated at 38 kHz ± 10 % with 110 W output power was used for sonication aid.

3. Results and discussion

3.1. Phytochemical analysis and antioxidant activity of P. Granatum

Although both varieties of *P. granatum* proved to possess polyphenols (Table 1), the Egyptian variety had relatively higher content of phenolics than Yemen variety (32.5 and 29.8 mg/g GAE). However, the Yemen variety showed higher flavonoids (4.8 and 4.7 mg/g QE) and significantly higher ($p < 0.05$) content of anthocyanins (2.18 μmole/g) as compared to the Egyptian variety (Table 1).

This high content of polyphenolics in both varieties was reflected in the reducing power (RP) and the DPPH radical scavenging activity of the extracts. Both varieties of *P. granatum* showed very high reducing power and free radical scavenging activity with a significant difference

Table 1
Phytochemical analysis of the EGY-PAM and YEM-PAM.

Secondary metabolites	EGY-PAM	YEM-PAM
Total phenolics (TP) mg GAE g^{-1} extract	32.5 ± 1.5^a	29.8 ± 1.45^a
Total flavonoids (TF) mg QE g^{-1} extract	4.7 ± 0.82^b	4.8 ± 1.4^b
Total anthocyanins μmole g^{-1} extract	0.96 ± 0.001^b	2.18 ± 0.02^a
RP at 1000 μg/ml (OD)	0.31 ± 0.004^a	0.28 ± 0.004^b
DPPH at 250 μg/ml)	83.3 ± 0.24^b	84.7 ± 0.0^b
IC_{50} of DPPH (μg mL^{-1})	113.1 ± 1.97^a	89.5 ± 6.43^a

GAE = gallic acid equivalent, QE = quercetin equivalent, RP = reducing power. Different letters in the same row means significant difference ($p < 0.05$) and the same letters means there is no significant difference.

between the Egyptian and Yemeni varieties regarding RP, whereas no significant difference between the Egyptian and Yemeni variety regarding DPPH was recorded (Table 1). The high DPPH radical scavenging activity resulted to impact on the IC_{50} of the extracts, where the Egyptian and Yemeni varieties showed low IC_{50} (113.1 and 89.5 μg/mL), respectively (Table 1 and Fig. 1). The IC_{50} of both varieties showed no significant difference at $p < 0.05$.

The increasing of reducing power with increasing the concentration of the extract in both *P. granatum* varieties indicates that these extracts have electron donor compounds that have the ability to convert the free radicals into stable products and prevent the radical chain reaction [33]. The antioxidant activity of *P. granatum* was previously reported and correlated to the presence of polyphenols [55] as similar the case for high content of flavonoids that was previously linked to the hydroxyl free radical scavenging activity [20].

3.2. Characterization of the as-prepared ZnO NPs

The XRD pattern of the developed ZnO NPs is illustrated in Fig. 2A. The diffraction peaks assigned at 2θ = 31.63°, 34.36°, 36.12°, 47.68°, 56.64°, 62.81°, 66.24°, 67.84°, 68.96°, 72.41° and 77.15° assure that the prepared ZnO is matched to JCPDS No. 36–1451 corresponding to the hexagonal wurtzite crystallinity and corresponds respectively to the

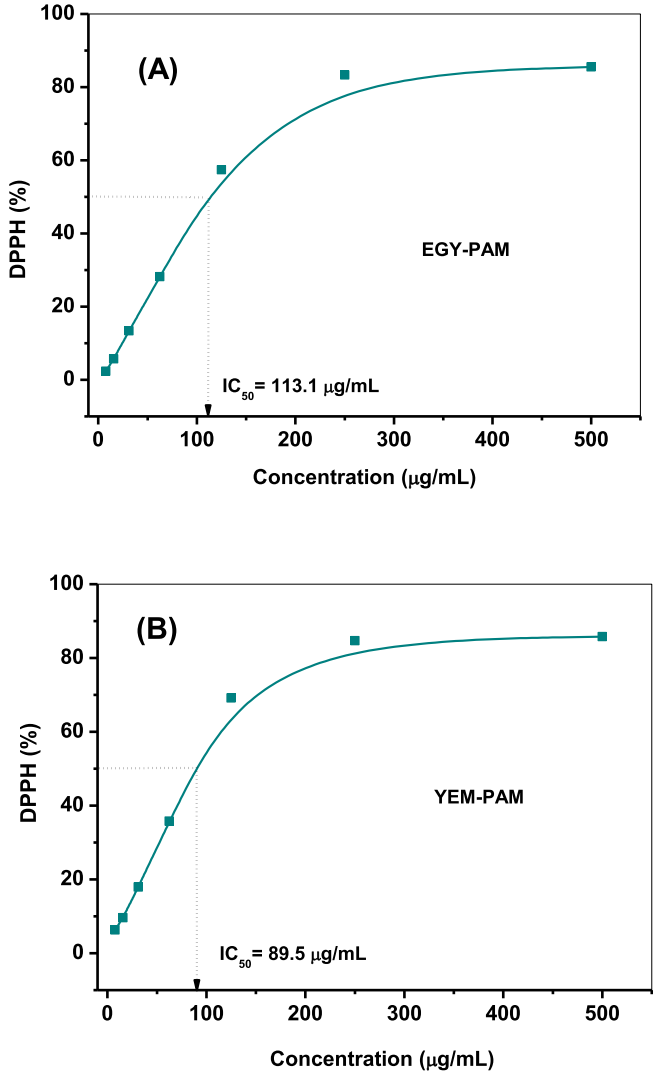

Fig. 1. The DPPH radical scavenging activity of EGY-PAM (A); and YEM-PAM (B).

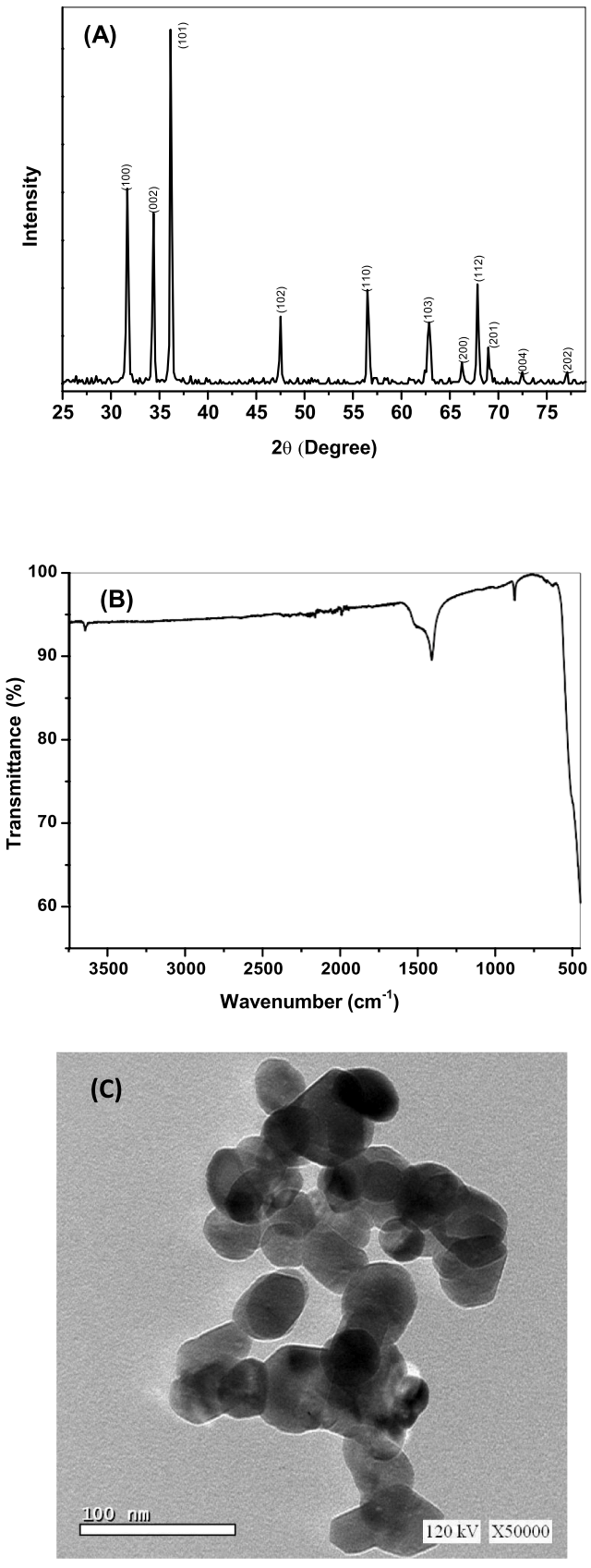

Fig. 2. Characterization of the developed ZnO NPs as revealed from analyses of (A) XRD pattern; (B) FTIR spectral data; (C) TEM morphological features.

crystal faces (100), (002), (101), (102), (110), (103), (200), (112), (201), (004) and (202). The relatively high ultrasound-mediated irradiation during the synthesis of ZnO could be responsible for the high purity obtained for ZnO. Under higher ultrasound irradiation, the by-product is destroyed, resulting in this phenomenon [17].

Moreover, the size of the crystallite (D) could be estimated from the Debye-Scherrer equation:

$$D = k\,\lambda/\beta\,\cos\theta \quad (4)$$

where k is of value 0.89 and refers to the Scherrer's constant, λ is X-ray wavelength ($\lambda = 1.54056$ Å), θ is the Bragg's angle, and β refers to the full width of the estimated peak at its half maximum. Hence, the average size of crystallite is estimated to be 26.3 nm.

As ascribed in Fig. 2B, the FTIR spectrum of the developed ZnO NPs was recorded from 400 to 4000 cm^{-1}. As seen, several bands are assigned at 451, 873, 1408, 1510 and 3639 cm^{-1}. The peaks at 435 and 870 cm^{-1} refer to Zn-O stretching vibrational motion [56]. The band assigned at 1408 cm^{-1} could be due to atmospheric CO_2 that is adsorbed on ZnO surface. Also, there are very small amount of water moisture on the surface of ZnO as revealed from the bands at 1510 and 3639 cm^{-1} of very weak intensity as a result of bending and stretching vibration modes of water.

Transmission electron microscopy (TEM) was employed to explore the morphological features of the solvothermally/sonochemically developed ZnO NPs. The TEM image picked up as in Fig. 2C manifests the predominance of spherical/hemispherical particulation of ZnO within a few of a square and hexagonal shaped particulation. The size estimation ranging from 18.7 to 33.4 nm that is found comparable to

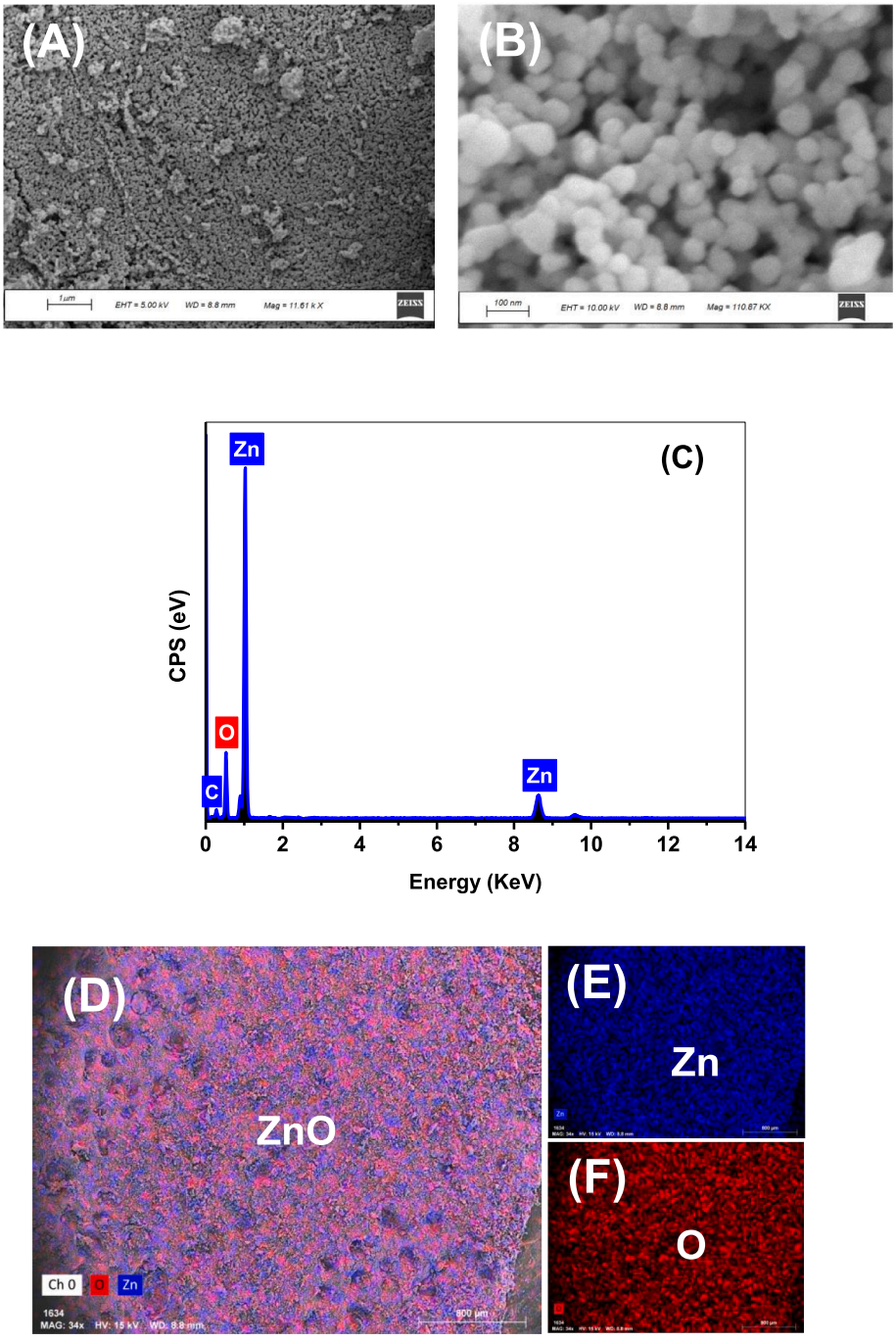

Fig. 3. SEM images at two magnifications (A) and (B); EDX spectrum (C) and EDX mapping (D–F) of the deveoped ZnO NPs.

that acquired for ZnO prepared under near ultrasonication conditions [17]. Under ultrasonication, the aggregation of the particles in the sample is reduced. For this sample, nanoparticle dispersal is dominated by microbubble formation and collapse [12,13].

SEM, EDX, and mapping were used to characterize Zn and O elements in the developed photocatalyst in order to better understand their distribution and content. As seen in Fig. 3, the distribution of ZnO particulates were highly uniform, with unconsiderable agglomeration of ZnO NPs, which was consistent with the TEM results. A further percentage of Zn and O were found to be 46.12 % and 53.8 %, respectively, in the EDX analysis results.

The UV– vis electronic spectroscopy of the developed ZnO NPs is illustrated in Fig. 4A. As shown there is a well-defined peak around 369 nm that is referred to the characteristic excitonic absorption and the surface Plasmon resonance of ZnO semiconductor nanoparticles. Furthermore, addressing of absorption features and the band gap of the developed ZnO is estimated from the Kubelka-Munk plotting:

$$(\alpha h\nu) = A\ (h\nu - E_g)^{1/2} \quad (5)$$

where h is Planck's constant, A refers to an absorption constant, α is extinction coefficient, E_g is the energy gap in eV, and ν is the frequency. When $(\alpha h\nu)^{1/2}$ extrapolating linearly versus (hν), E_g of estimate 3.32 eV is obtained (Fig. 4B).

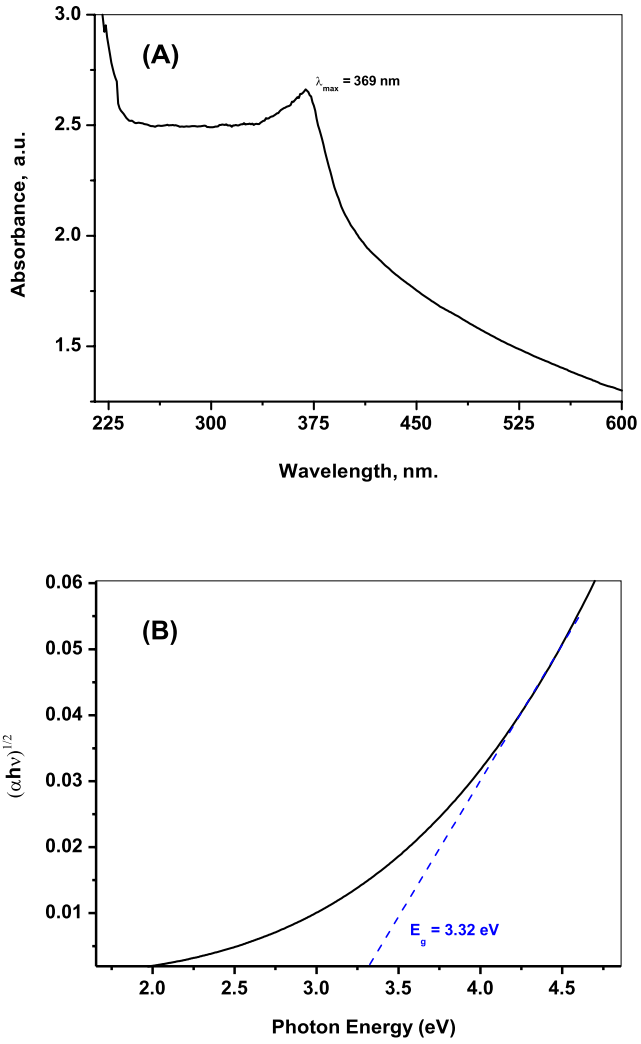

Fig. 4. UV–Vis electronic spectra (A); and The plot of $(\alpha h\upsilon)^{1/2}$ versus hυ for the developed ZnO NPs.

3.3. Solar-driven photocatalytic activity of ZnO NPs in breeding hydroxyl radicals (˙OH) and their selective photoluminescence monitoring

The efficacy of the developed ZnO NPs in breeding ˙OH radicals after its subjecting to solar irradiation was estimated via the sensitively selective photoluminescence (PL) approach using the terephthalic acid (TA)/NaOH probe [55]. As shown in Fig. 5A, photo-illuminating the developed ZnO NPs semiconductor reveals electronic excitation from the valence band (VB) to the conduction band (CB) leaving behind the photogenerated holes (h^+). These holes were interacted with water molecules breeding the ˙OH radicals. These nascent ˙OH radicals were selectively tapped by the non-fluorescent terephthalate system forming the strongly fluorescent hydroxy terephthalate with a characteristic emission signal at λ_{em} = 426 nm., Fig. 5B. Along 80 min. of Solar-illuminating ZnO NPs, a noticeable increase in the fluorescence intensity of the formed hydroxy terephthalate fluorophore [57] is recorded as a result of higher concentration of produced ˙OH radicals (Fig. 5B). A control experiment for examining the influence of solar-irradiating TA/NaOH solution in absence of ZnO NPs reveals that no

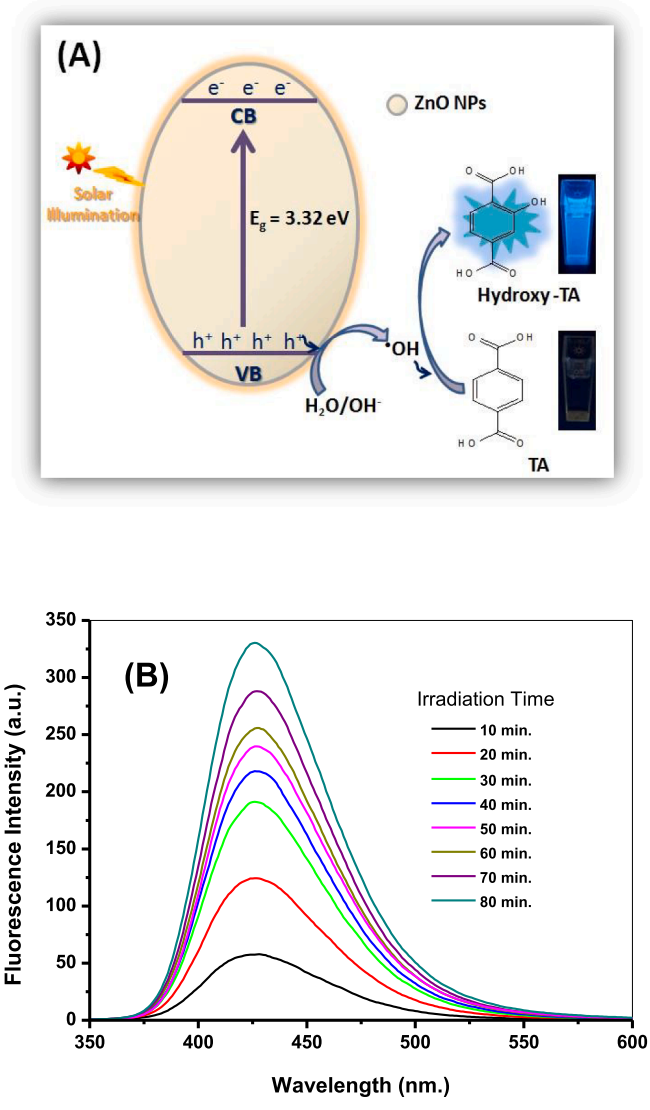

Fig. 5. Illustrative Scheme for the ˙OH radicals productivity via the suited solar-driven catalytic photoexcitation of the synthesized ZnO NPs (A); Fluorescence spectra of hydroxy terephthalate fluorophore (λ_{ex} = 315 nm) due to ˙OH-trapping during 80 min. of sunlight-illumination of the synthesized ZnO NPs (B).

hydroxy terephthalate was generated [28].

3.4. Spectrofluorimetric assessment of EGY-PAM or YEM-PAM efficacies in scavenging ˙OH radicals.

The aforementioned fluorimetric probing in section 3.3 was employed in presence of different dosages (90, 110, 155, and 220 μg/mL) of either EGY-PAM or YEM-PAM samples to examine their activities in scavenging ˙OH radicals. Fig. 6 shows the temporal variations in fluorescence intensities of the formed hydroxyl terephthalate along 80 min. of solar-illuminating ZnO NPs in presence of 90 and 220 μg/mL of EGY-PAM or YEM-PAM. As seen, the characteristic fluorescent signal depicted for the trapping of ˙OH radicals exhibited noticeably decreased intensity with different degrees. Addition of 90 μg/mL from EGY-PAM or YEM-PAM decreases the Max I_f from 331.9 in blank experiment to 261.4 and 292.2, corresponding to 21.6 and 11.6 % ˙OH scavenging, respectively. While adding maximum dose of 220 μg/mL from EGY-PAM or YEM-PAM sharply declines the Max I_f to 44.7 and 50.8 corresponding to 87 and 84 % ˙OH scavenging, respectively. The estimated ˙OH % scavenging due to the different doses from EGY-PAM or YEM-PAM and the TBHQ synthetic antioxidant (200 μg/mL) are compared as shown in Fig. 7A and Table 2. Comparison clearly illustrates the superior potentiality of EGY-PAM in scavenging ˙OH radicals over YEM-PAM especially at low dosage in addition to the interesting performance of either EGY-PAM or YEM-PAM at 220 μg/mL in scavenging ˙OH radicals by 87 and 84 %, respectively that are significant higher than TBHQ at dosage 200 μg/mL. Moreover, closer comparison for the performance of either EGY-PAM or YEM-PAM in scavenging ˙OH radicals is clearly addressed from the estimated values of IC_{50}. As seen in Fig. 7B, the values of IC_{50} for EGY-PAM and YEM-PAM are 105.7 and 153.4 μg/mL significantly refers to the superiority of EGY-PAM over YEM-PAM in scavenging ˙OH.

Furthermore, the antioxidant efficacy of EGY-PAM and YEM-PAM were kinetically examined by comparing the rates of breeding ˙OH radicals in absence and presence of antioxidant samples. Fig. 8,9 compare the kinetics of producing ˙OH radicals in presence of different doses from EGY-PAM or YEM-PAM and TBHQ (200 μg/mL). As seen, by increasing the added concentration from EGY-PAM or YEM-PAM, the kinetic patterns for breeding ˙OH radicals decreases from 0.07 min^{-1} in blank experiment to 0.031 $min^{-1}$and 0.053 min^{-1}, respectively versus 0.049 min^{-1} when adding TBHQ. This is another confirmation for the higher efficacy of EGY-PAM as antioxidant over YEM-PAM. This could be attributed to the higher reducing power and the higher content of the phenolics secondary metabolites in the EGY-PAM rather than YEM-PAM as previously illustrated in Table 1.

3.5. Fluorimetric assessment of the ˙OH radicals scavenging potentiality of EGY-PAM or YEM-PAM in presence of glucose or NaCl

Moreover, the efficacy of EGY-PAM and YEM-PAM antioxidants in scavenging ˙OH radicals was further examined in presence of high levels of glucose (5 mg/mL) and NaCl (15 mg/mL) as a common existing compounds, respectively in case of patients of diabetes and high blood pressure diseases. But firstly, it is necessary to preliminary examine the effect of adding either glucose or NaCl to the fluorescence intensity of already formed hydroxy terephthalate fluorphore in absence of EGY-PAM and YEM-PAM. The recorded fluorescence intensities of hydroxy terephthalate are found to be insignificantly influenced by adding either glucose or NaCl confirming the preciseness of the ˙OH radicals probing technicality. The results depicted in Fig. 10 estimated from the comparison of fluorescence intensities (λ_{em} 426 nm.) due to 80 min. of solar-irradiation for ZnO/TA/NaOH/antioxidant probing system in absence and presence of glucose or NaCl. The results show a retardation in the ˙OH radicals scavenging percentage of EGY-PAM by 3.6 % and 11.8 % in presence of glucose or NaCl, respectively. In case of YEM-PAM, the ˙OH radicals scavenging percentage was retarded by 13.6 % and 5 % when adding respectively, glucose and NaCl to the working system. Such reverse potentialities of EGY-PAM and YEM-PAM in the ˙OH radicals scavenging performance when adding either glucose or NaCl may be

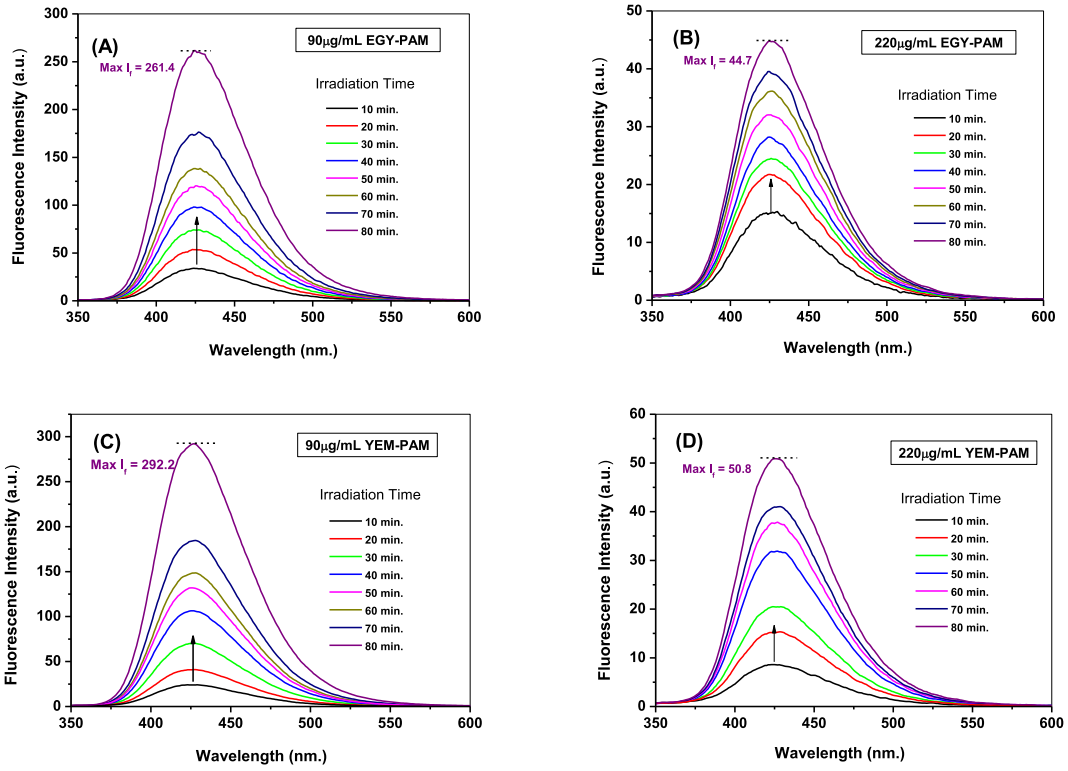

Fig. 6. Temporal variations in fluorescence intensities of the formed hydroxyl terephthalate due to nascent generative ˙OH radicals via solar-illuminated ZnO NPs in presence of (A) 90 μg/mL EGY-PAM; (B) 220 μg/mL EGY-PAM; (C) 90 μg/mL YEM-PAM; (D) 220 μg/mL YEM-PAM.

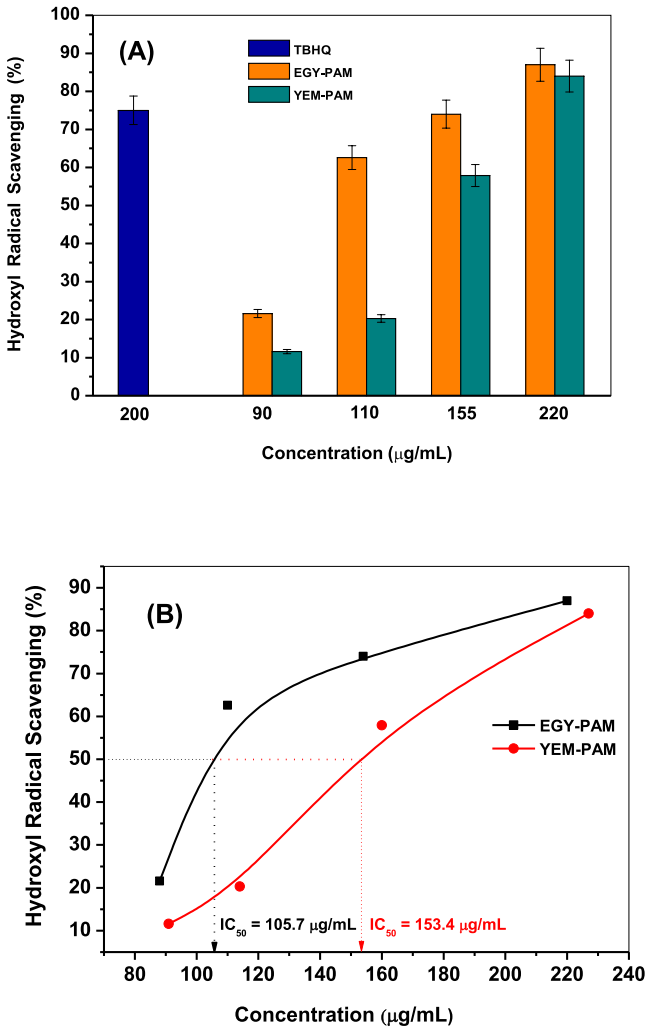

Fig. 7. Hydroxyl radicals scavenging(%) due to different concentrations (90, 110, 155, 220 μg/mL) of EGY-PAM and YEM-PAM in comparison with TBHQ antioxidant (200 μg/mL) (A); Hydroxyl radicals scavenging in terms of IC_{50} for EGY-PAM and YEM-PAM (B).

Table 2
The estimates of hydroxyl radicals scavenging(%) and first-order rate constant for breeding hydroxyl radicals for EGY-PAM and YEM-PAM in comparison to TBHQ.

Sample	Concentration (μg/mL)	˙OH radicals scavenging (%)	Rate of ˙OH radicals productivity ($min.^{-1}$)	R^2
EGY-PAM	90	21.6	–	–
	110	62.6	–	–
	155	74	–	–
	220	87	0.0312	0.96
YEM-PAM	90	11.6	–	–
	110	20.3	–	–
	155	57.9	–	–
	220	84	0.053	0.93
TBHQ	200	75	0.049	0.92

attributed to the variations in the formulations of their active constituents.

3.6. Anti-proliferative activity

The ethanol extract of both extracts of *P. granatum* (the Egyptian and Yemeni) proved to have strong antiproliferative activity against two

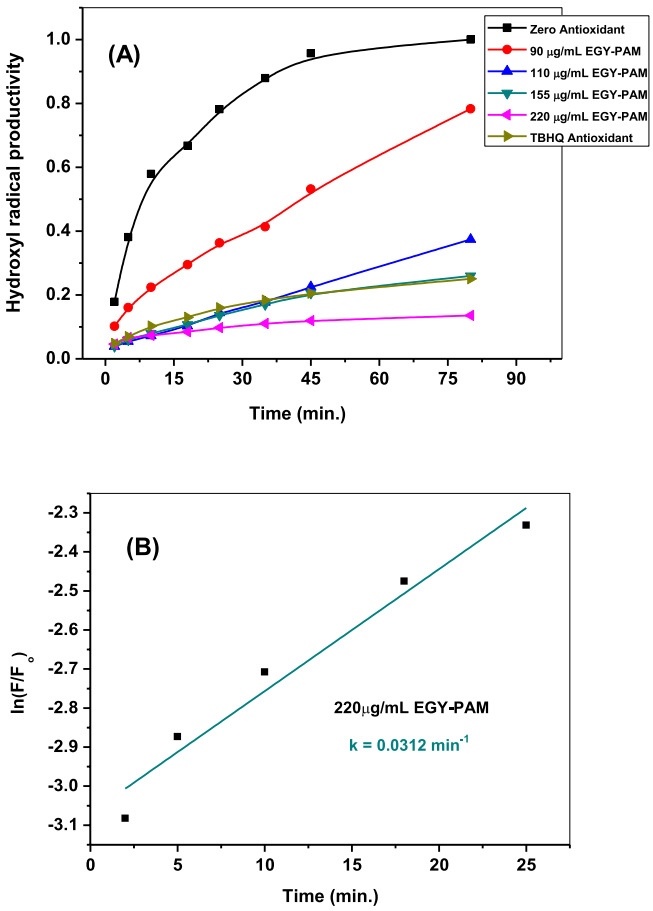

Fig. 8. The kinetics of breeding ˙OH radicals in absence and presence of different concentrations from EGY-PAM in comparison to TBHQ (A); Estimation of first order rate constant in breeding ˙OH radicals in presence of EGY-PAM (220 μg/mL).

cancer cell lines: hepatocellular carcinoma (Hep-G2) and breast cancer cell lines (MCF7). Among these, MCF7 showed more resistance as compared with Hep-G2, against both *P. granatum* extracts. The Egyptian *P. granatum* extract showed very low IC_{10} with Hep-G2 and MCF7 (1.19 and 3.52 μg/mL), respectively. The Yemeni *P. granatum* extract showed higher IC_{10} than the Egyptian one with Hep-G2 and MCF7 (1.98 and 4.08 μg/mL), respectively (Fig. 11A,B). The anti-proliferative activity of *P. granatum* extracts may be attributed to not only the high content of the secondary metabolites contributing to anticancer activity, such as phenolics, flavonoid, and anthocyanins, but also to other secondary metabolites which have not been determined in this study. The anti-proliferative activity of the ethanol extracts of some Asteraceae plants growing in Saudi Arabia against Hep-G2 and MCF7 was attributed to the high contents of phenolics and flavonoids [54]. Moreover, *Zea mays* anthocyanins exerted anti-proliferative activity against colon cancer cell lines [58]. Polyphenols as well as phenolics-rich extracts showed anti-proliferative activity against hepatocellular carcinoma and colon cancer cell lines in vitro and *in vivo* [59,60].

4. Conclusion

Hybrid solvothermal/sonochemical route was used to prepare ZnO NPs that were characterized by XRD, FTIR, TEM, SEM, EDX and UV–vis. spectrophotometry analyses. Ultrasound-mediated irradiation may be responsible for ZnO's high purity. As the ultrasonic irradiation can destroy the by-product, hence possibly responsible for this phenomenon. The XRD diffractogram indicated high crystallinity within hexagonal wurtzite crystal faces. TEM image showed the predominance of

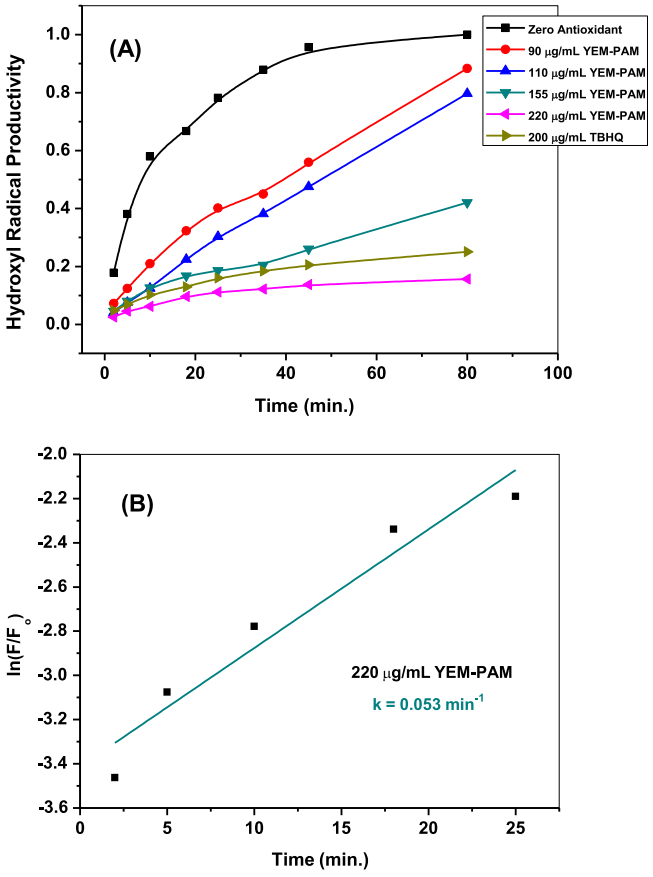

Fig. 9. The kinetics of breeding ˙OH radicals in absence and presence of different concentrations from YEM-PAM in comparison to TBHQ (A); Estimation of first order rate constant in breeding ˙OH radicals in presence of YEM-PAM (220 μg/mL).

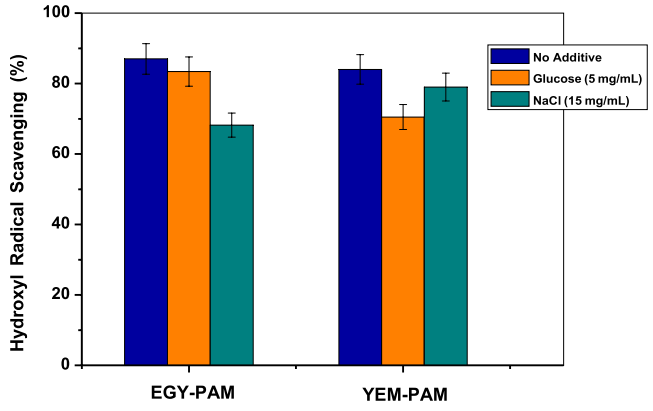

Fig. 10. Efficacy of EGY-PAM and YEM-PAM antioxidants in scavenging ˙OH radicals was in presence of glucose (5 mg/mL) and NaCl (15 mg/mL).

spherical/hemispherical particulation with size estimates ranging from 18.7 to 33.4 nm where ultrasound reduced sample particle aggregation. In this sample, microbubble formation and collapse dominated nanoparticle dispersal. The SEM, EDX, and mapping were used to characterize Zn and O in the developed photocatalyst where ZnO particulates were highly uniform with little agglomeration, consistent with TEM results. The EDX analysis found 46.12 % Zn and 53.8 % O. Solar –illumination of the developed ZnO NPs produced high density of hydroxyl radicals (˙OH) as monitored by fluorimetric probing. Accordingly, and for the first time, a sensitive/selective photoluminescent

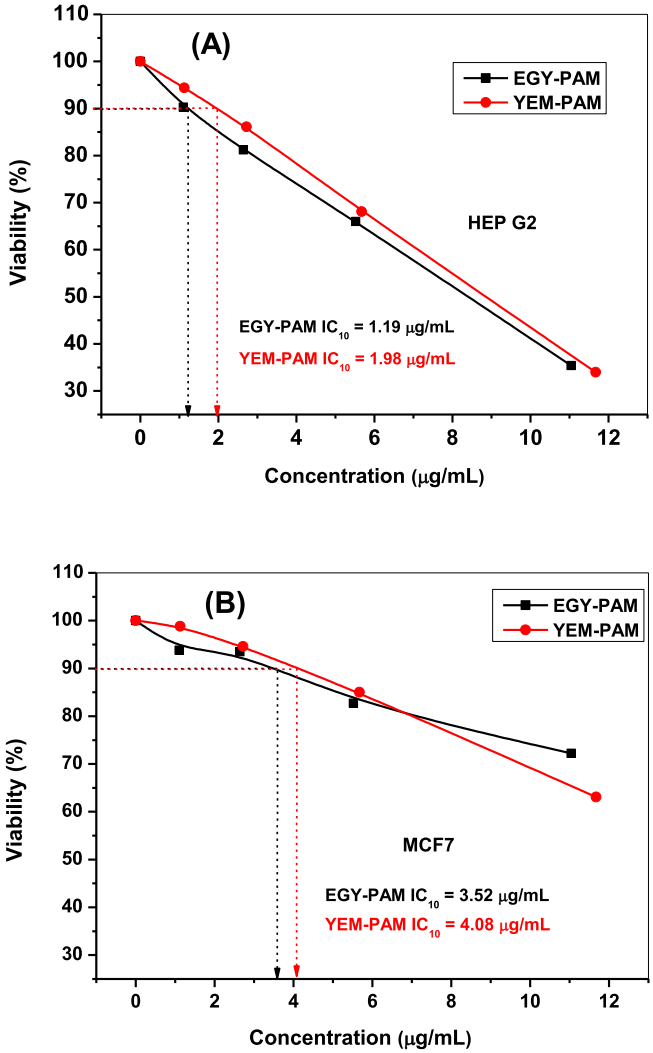

Fig. 11. Antiproliferative activity of EGY-PAM and YEM-PAM against two cancer cell lines: hepatocellular carcinoma (Hep-G2) (A); and breast cancer cell lines (MCF7) (B).

avenue was framed to evaluate the ˙OH scavenging activity of Egyptian and Yemeni varieties from *P. granatum* (EGY-PAM, YEM-PAM). Phytochemical analysis of EGY-PAM and YEM-PAM detectd high content of total phenolics, total flavonoids, and anthocyanins that reflected to the high %DPPH radical scavenging. The traditional DPPH radical scavenging methodology could not show the significant difference in spite of the superior content of phenolics in the EGY-PAM rather than YEM-PAM. Unlike, the developed fluorimetric probing, sensitively discriminated the ˙OH scavenging activities of EGY-PAM and YEM-PAM. These results are compatible with the higher reducing power of EGY-PAM than YEM-PAM and interestingly superior to the TBHQ synthetic antioxidant. Moreover, the efficacy of EGY-PAM and YEM-PAM antioxidants in scavenging ˙OH radicals was further examined in presence of high levels of glucose and NaCl. Surprisingly, the ˙OH scavenging activity of the developed EGY-PAM and YEM-PAM are comparable to the synthetic antioxidant TBHQ and still viable in presence of high dosage from glucose or NaCl. EGY-PAM may be recommended as ˙OH radicals scavenger for diabetic patients while YEM-PAM exhibits a better ˙OH radicals scavenging appropriate for high blood pressure patients. More interestingly, the ˙OH scavenging activities as well as the anticancer potentiality addressed for EGY-PAM and YEM-PAM make them a promising source of natural antioxidants that will preserve their activity even when dealing with chronic diseases like diabetes and high blood pressure as

well as cancer therapeutic protocols. This encourages the future inaugurating of EGY-PAM and YEM-PAM as a potent therapeutic agent in free radical induced diseases.

CRediT authorship contribution statement

Amr A. Essawy: Conceptualization, Methodology, Software, Validation, Formal analysis, Investigation, Resources, Data curation, Writing – original draft, Writing – review & editing, Visualization, Supervision, Project administration, Funding acquisition. **Ibrahim B. Abdel-Farid:** Methodology, Validation, Resources, Data curation, Writing – review & editing, Supervision, Project administration, Funding acquisition.

Declaration of Competing Interest

The authors declare that they have no known competing financial interests or personal relationships that could have appeared to influence the work reported in this paper.

Data availability

Data will be made available on request.

References

[1] A.A. Essawy, S.M. Sayyah, A.M. El-Nggar, Ultrasonic-mediated synthesis and characterization of TiO_2-loaded chitosan-grafted polymethylaniline nanoparticles of potent efficiency in dye uptake and sunlight driven self cleaning applications, RSC Adv. 6 (2016) 2279, https://doi.org/10.1039/C5RA20343K.

[2] A.A. Essawy, S.M. Sayyah, A.M. El-Nggar, Wastewater remediation by TiO_2-impregnated chitosan nano-grafts exhibited dual functionality: High adsorptivity and solar-assisted self-cleaning, J. Photochem. Photobiol. B: Biol 173 (2017) 170–180, https://doi.org/10.1016/j.jphotobiol.2017.05.044.

[3] A.A. Essawy, A.M. Nassar, W.A.A. Arafa, A novel photocatalytic system consists of Co(II) complex@ZnO exhibits potent antimicrobial activity and efficient solar-induced wastewater remediation, Sol. Energy 17 (2018) 388–397, https://doi.org/10.1016/j.solener.2018.05.073.

[4] A.A. Essawy, I.H. Alsohaimi, M.S. Alhumaimess, H.M.A. Hassan, M.M. Kamel, Green synthesis of spongy Nano-ZnO productive of hydroxyl radicals for unconventional solar-driven photocatalytic remediation of antibiotic enriched wastewater, J. Environ. Manage. 271 (2020), 110961.

[5] Z.A. Alrowaili, I.H. Alsohaimi, M.A. Betiha, A.A. Essawy, A.A. Mousa, S. F. Alruwaili, H.M.A. Hassan, Green fabrication of silver imprinted titania/silica nanospheres as robust visible light-induced photocatalytic wastewater purification, Mater. Chem. Phys. 241 (2020), 122403.

[6] M.S. Alshammari, A.A. Essawy, A.M. El-Nggar, S.M. Sayyah, Ultrasonic-assisted synthesis and characterization of chitosan-graft-substituted polyanilines: promise bio-based nanoparticles for dye removal and bacterial disinfection, J. Chem. (2020), https://doi.org/10.1155/2020/3297184.

[7] S.S. Alias, A.B. Ismail, A.A. Mohamad, Effect of pH on ZnO nanoparticle properties synthesized by sol–gel centrifugation, J. Alloy. Compd. 499 (2011) 231–237.

[8] D. Sharma, R. Jha, Structural and optical properties of Co-doped ZnO nano-ampoules synthesized by co-precipitation method, Mater. Lett. 190 (2017) 9–12.

[9] M. Jamshidi, M. Ghaedi, K. Dashtian, S. Hajati, A.A. Bazrafshan, Sonochemical assisted hydrothermal synthesis of ZnO: Cr nanoparticles loaded activated carbon for simultaneous ultrasound-assisted adsorption of ternary toxic organic dye: Derivative spectrophotometric, optimization, kinetic and isotherm study, Ultrason. Sonochem. 32 (2016) 119–131.

[10] S.D. Birajdara, V.R. Bhagwatb, A.B. Shindec, K.M. Jadhava, Effect of Co^{2+} ions on structural, morphological and optical properties of ZnO nanoparticles synthesized by sol–gel auto combustion method, Mat. Sci. Semicn. Proc. 41 (2016) 441–449.

[11] Y. Wu, X. Liu, X. Bai, W. Wu, Ultrasonic-assisted preparation of ultrafine Pd nanocatalysts loaded on Cl- intercalated MgAl layered double hydroxides for the catalytic dehydrogenation of dodecahydro-N-ethylcarbazole, Ultrason. Sonochem. 88 (2022), 106097.

[12] Y.H. Shih, C.Y. Hsu, Y.F. Su, Reduction of hexachlorobenzene by nanoscale zero-valent iron: Kinetics, pH effect, and degradation mechanism, Sep. Purif. Technol. 76 (2011) 268–274.

[13] K. Darko-Kagya, A.P. Khodadoust, K.R. Reddy, Reactivity of lactate-modified nanoscale iron particles with 2,4-dinitrotoluene in soils, J. Hazard. Mater. 182 (2010) 177–183.

[14] T.V.L. Thejaswini, D. Prabhakaran, M. Akhila Maheswari, Ultrasound assisted synthesis of nano-rod embedded petal designed α-Bi_2O_3-ZnO nanoparticles and their ultra-responsive visible light induced photocatalytic properties, J. Photochem. Photobiol., A 335 (2017) 217–229.

[15] R.M. Mohamed, D.L. McKinney, W.M. Sigmund, Enhanced nanocatalysts, Mater. Sci. Eng., R 73 (2012) 1–13.

[16] Z. Sharifalhoseini, M.H. Entezari, R. Jalal, Direct and indirect sonication affect differently the microstructure and the morphology of ZnO nanoparticles: Optical behavior and its antibacterial activity, Ultrason. Sonochem. 27 (2015) 466–4733.

[17] R. Mahdavi, S.S.A. Talesh, The effect of ultrasonic irradiation on the structure, morphology and photocatalytic performance of ZnO nanoparticles by sol-gel method, Ultrason. Sonochem. 39 (2017) 504–510.

[18] M. Mittal, M.R. Siddiqui, K. Tran, S.P. Reddy, A.B. Malik, Reactive oxygen species in inflammation and tissue injury, Antioxid. Redox. Sign. 2014 (20) (2014) 1126–1167, https://doi.org/10.1089/ars.2012.5149.

[19] J.T. Hou, M. Zhang, Y. Liu, X. Ma, R. Duan, X. Cao, F. Yuan, Y.X. Liao, W.S. Wang, W.X. Ren, Fluorescent detectors for hydroxyl radical and their applications in bioimaging: A review, Coord. Chem. Rev. 421 (2020), 213457, https://doi.org/10.1016/j.ccr.2020.213457.

[20] J. Treml, K. Smejkal, Flavonoids as potent scavengers of hydroxyl radicals, Compr. Rev. Food Sci. Food Saf. 15 (2016) 720–738, https://doi.org/10.1111/1541-4337.12204.

[21] A. Catala, A synopsis of the process of lipid peroxidation since the discovery of the essential fatty acids, Biochem. Biophys. Res. Commun. 399 (2010) 318–323, https://doi.org/10.1016/j.bbrc.2010.07.087.

[22] M.D. Evans, M. Dizdaroglu, M.S. Cooke, Oxidative DNA damage and disease: induction, repair and significance, Mutat. Res. 567 (2004) 1–61, https://doi.org/10.1016/j.mrrev.2003.11.001.

[23] B. Bekdeşer, M. Özyürek, K. Güclü, R. Apak, Novel spectroscopic sensor for the hydroxyl radical scavenging activity measurement of biological samples, Talanta 99 (2012) 689–696, https://doi.org/10.1016/j.talanta.2012.07.004.

[24] Y.Z. Xian, M.C. Liu, Q. Cai, H. Li, J. Lu, L. Jin, Preparation of microporous aluminium anodic oxide film modified Pt nano array electrode and application in direct measurement of nitric oxide release from myocardial cells, Analyst 126 (6) (2001) 871–876, https://doi.org/10.1039/b010181h.

[25] C. Oh, M. Li, E.H. Kim, J. Seok Park, J.C. Le, H.S. Wook, Bull. Korean Chem. Soc. 31 (12) (2010) 3513–3514, https://doi.org/10.5012/bkcs.2010.31.12.3513.

[26] T. Oka, S. Yamashita, M. Midorikawa, S. Saiki, Y. Muroya, M. Kamibayashi, Y. Katsumura, Spin-trapping reactions of a novel gauche type radical trapper G-CYPMPO, Anal. Chem. 83 (2011) 9600–9604, https://doi.org/10.1021/ac2023926.

[27] H.Y. Choi, J.H. Song, D.K. Park, A combined flow injection-chemiluminescent method for the measurement of radical scavenging activity, Anal. Biochem. 264 (1998) 291–293, https://doi.org/10.1006/abio.1998.2864.

[28] M.E. Lindsey, M.A. Tarr, Inhibition of hydroxyl radical reaction with aromatics by dissolved natural organic matter, Environ. Sci. Technol. 34 (2000) 444–449, https://doi.org/10.1021/es990457c.

[29] G. Žerjav, A. Albreht, I. Vovk, A. Pintar, Revisiting terephthalic acid and coumarin as probes for photoluminescent determination of hydroxyl radical formation rate in heterogeneous photocatalysis, Appl. Catal. A 598 (2020), 117566, https://doi.org/10.1016/j.apcata.2020.117566.

[30] B. Tang, L. Zhang, Y. Geng, Determination of the antioxidant capacity of different food natural products with a new developed flow injection spectrofluorimetry detecting hydroxyl radicals, Talanta 65 (2005) 769–775, https://doi.org/10.1016/j.talanta.2004.08.004.

[31] K. Li, L.L. Li, Q. Zhou, K.K. Yu, J.S. Kim, X.Q. Yu, Reaction-based fluorescent probes for SO_2 derivatives and their biological applications, Coord. Chem. Rev. 388 (2019) 310–333, https://doi.org/10.1016/j.ccr.2019.03.001.

[32] X. Liu, N. Li, M. Li, H. Chen, N. Zhang, Y. Wang, K. Zheng, Recent progress in fluorescent probes for detection of carbonyl species: Formaldehyde, carbon monoxide and phosgene, Coord. Chem. Rev. 404 (2020), 213109, https://doi.org/10.1016/j.ccr.2019.213109.

[33] M. Gupta, U.K. Mazumder, P. Gomathi, Evaluation of antioxidant and free radical scavenging activities of *Plumeria acuminate* leaves, J. Biol. Sci. 7 (8) (2007) 1361–1367, https://doi.org/10.3923/jbs.2007.1361.1367.

[34] H. Wiseman, B. Halliwell, Damage to DNA by reactive oxygen and nitrogen species: role in inflammatory disease and progression to cancer, Biochem. J. 313 (1) (1996) 17–29, https://doi.org/10.1042/bj3130017.

[35] Y.X. Sun, J.F. Kennedy, Antioxidant activities of different polysaccharide conjugates (CRPs) isolated from the fruiting bodies of *Chroogomphis rutilus* (Schaeff.: Fr.) D. K. Miller, Carbohydr. Polym. 82 (2) (2010) 510–514, https://doi.org/10.1016/j.carbpol.2010.05.010.

[36] Y. Zou, Y. Zhao, W. Hu, Chemical composition and radical scavenging activity of melanin from Auricularia auricula fruiting bodies, Food Sci. Technol. 35 (2) (2015) 253–258, https://doi.org/10.1590/1678-457X.6482.

[37] V.A. Evreinoff, Le grenadier, Fruits d'Outre-Mer 4 (5) (1949) 161–170.

[38] J. Tous, L. Ferguson, Mediterranean fruits, in: J. Janick (Ed.), Progress in New Crops, ASHS Press, Arlington, VA, USA, 1996, pp. 416–430.

[39] N. Hasnaoui, M. Mars, J. Chibani, M. Trifi, Molecular polymorphisms in Tunisian pomegranate (*Punica granatum* L.) as revealed by RAPD fingerprints, Diversity. 2 (1) (2010) 107–114, https://doi.org/10.3390/d2010107.

[40] T. Ablola, L.K. Falana, D.O. Adediji, Proximate composition, phytochemical analysis and in vivo antioxidant activity of pomegranate seeds (*Punica granatum*) in female albino mice Biochem, Pharmacol. 7 (2) (2018) 1–6, https://doi.org/10.4172/2167-0501.1000250.

[41] A.A. Al-Huqail, G.A. Elgaaly, M.M. Ibrahim, Identification of bioactive phytochemical from two *Punica* species using GC–MS and estimation of antioxidant activity of seed extracts, Saudi J. Biol. Sci. 25 (7) (2018) 1420–1428, https://doi.org/10.1016/j.sjbs.2015.11.009.

[42] S.I. Ali, F.K. El-Baz, G.A. El-Emary, E.A. Khan, A.A. Mohamed, HPLC-analysis of polyphenolic compounds and free radical scavenging activity of pomegranate fruit (*Punica granatum* L.), Int. J. Pharm. Clin. Res. 6 (4) (2014) 348–355.

[43] A.S. Al-Rawahi, G. Edwards, M. Al-Sibani, G. Al-Thani, A.S. Al-Harrasi, M. S. Rahman, Phenolic constituents of pomegranate peels (*Punica granatum* L.) cultivated in Oman, Eur. J. Med. Plants 4 (3) (2014) 315–331, https://doi.org/10.9734/EJMP/2014/6417.
[44] G. Hernández Escarcega, E. Sánchez-Chávez, S. Pérez Álvarez, M. Soto Caballero, J. M. Soto Parra, M.A. Flores-Córdova, N.A. Salas Salazar, D.L. Ojeda Barrios, Determination of antioxidant phenolic, nutritional quality and volatiles in pomegranates (*Punica granatum* L.) cultivated in Mexico, Int. J. Food Prop. 23 (1) (2020) 979–991, https://doi.org/10.1080/10942912.2020.1760879.
[45] P. Melgarejo-Sánchez, D. Núñez-Gómez, J.J. Martínez-Nicolás, F. Hernández, P. Legua, P. Melgarejo, Pomegranate variety and pomegranate plant part, relevance from bioactive point of view: a review, Bioresour. Bioprocess. 8 (1) (2021) 1–29, https://doi.org/10.1186/s40643-020-00351-5.
[46] A.M. Tamamm, S.M. El-Sonbaty, F.S. Moawed, E.I. Kandil, Antitumor efficacy of ellagic acid against MCF-7 using nanotechnology, Nat. Sci. 16 (2018) 44–47, https://doi.org/10.7537/marsnsj161118.06.
[47] M. Suman, B. Prerak, A review on proactive pomegranate one of the healthiest foods, Int. J. Chem. Stud. 7 (3) (2019) 189–194.
[48] V.L. Singleton, R. Orthofer, R.M. Lamuela-Raventos, Analysis of total phenols and other oxidation substrates and antioxidants by means of Folin-Ciocalteau reagent, Methods Enzymol. 299 (1999) 152–178, https://doi.org/10.1016/S0076-6879(99)99017-1.
[49] J. Zhishen, T. Mengcheng, W. Jianming, The determination of flavonoid contents in mulberry and their scavenging effects on superoxide radicals, Food Chem. 64 (4) (1999) 555–559, https://doi.org/10.1016/S0308-8146(98)00102-2.
[50] M. Padmavati, N. Sakthivel, K.V. Thara, A.R. Reddy, Differential sensitivity of rice pathogens to growth inhibition by flavonoids, Phytochemistry 46 (1997) 499–502, https://doi.org/10.1016/S0031-9422(97)00325-7.
[51] M. Oyaizu, Studies on products of browning reaction—antioxidative activities of products of browning reaction, Jpn. J. Nutr. 44 (1986) 307–315, https://doi.org/10.5264/eiyogakuzashi.44.307.
[52] M.S. Blois, Antioxidant determinations by the use of a stable free radical, Nature 181 (1958) 1199–1200, https://doi.org/10.1038/1811199a0.
[53] V. Vichai, K. Kirtikara, Sulforhodamine b colorimetric assay for cytotoxicity screening, Nat. Protoc. 1 (2006) 1112–1116, https://doi.org/10.1038/nprot.2006.179.
[54] S.A. El-Naggar, I.B. Abdel-Farid, H.A. Elgebaly, M.O. Germoush, Metabolomic profiling, antioxidant capacity and in vitro anticancer activity of some compositae plants growing in Saudi Arabia, Afr. J. Pharm. Pharmacol 9 (2015) 764–774.
[55] Y. Noda, T. Kaneyuki, A. Mori, L. Packer, Antioxidant activities of pomegranate fruit extract and its anthocyanidins: delphinidin, cyanidin, and pelargonidin, J. Agric. Food Chem. 50 (2002) 166–171, https://doi.org/10.1021/jf0108765.
[56] A.A. Essawy, Silver imprinted ZnO nanoparticles: Green synthetic approach, characterization and efficient sunlight-induced photocatalytic water detoxification, J. Clean. Prod. 183 (2018) 1011–1020, https://doi.org/10.1016/j.jclepro.2018.02.214.
[57] Y. Xu, H. Li, B. Sun, P. Qiao, L. Ren, M. Li, B. Jiang, K. Pan, W. Zhou, Surface oxygen vacancy defect-promoted electron hole separation for porous defective ZnO hexagonal plates and enhanced solar driven photocatalytic performance, Chem. Eng. J. 379 (2020), 122295, https://doi.org/10.1016/j.cej.2019.122295.
[58] X. Zhao, C. Zhang, C. Guigas, Y. Ma, M. Corrales, B. Tauscher, X. Hu, Composition, antimicrobial activity, and antiproliferative capacity of anthocyanin extracts of purple corn (Zea maysL.) from China, Eur. Food Res. Technol. 228 (2009) 59–765, https://doi.org/10.1007/s00217-008-0987-7.
[59] A.M. Mahmoud, E.M. Abdella, A.M. El-Derby, Protective effects of Turbinaria ornata and Padina pavonia against azoxymethane-induced colon carcinogenesis through modulation of ppar gamma, nf-kappab and oxidative stress, Phytother. Res. 29 (5) (2015) 737–748, https://doi.org/10.1002/ptr.5310.
[60] A.M. Mahmoud, M.Y. Alexander, Y. Tutar, F.L. Wilkinson, A. Venditti, Oxidative stress in metabolic disorders and drug-induced injury: The potential role of Nrf2 and PPARs activators, Oxid. Med. Cell. Longev 2508909 (2017), https://doi.org/10.1155/2017/2508909.